Geotechnical Safety and Risk IV – Zhang et al. (eds)

Homogenization of geomaterials using the random finite element method

D.V. Griffiths
Colorado School of Mines, Golden, CO, USA
University of Newcastle, NSW, Australia

Jumpol Paiboon
Colorado School of Mines, Golden, CO, USA

Jinsong Huang
University of Newcastle, NSW, Australia

Gordon A. Fenton
Dalhousie University, Halifax, NS, Canada

ABSTRACT: The homogenized stiffness of geomaterials that are highly variable at the micro-scale has long been of interest to geotechnical engineers. The purpose of this study is to investigate the influence of porosity and void size on the homogenized or effective properties of geomaterials. A Random Finite Element Method (RFEM) has been developed enabling the generation of spatially random voids of given porosity and size within a block of geomaterial. Following Monte-Carlo simulations, the mean and standard deviation of the effective property can be estimated leading to a probabilistic interpretation involving deformations. The probabilistic approach represents a rational methodology for guiding engineers in the risk management process. The influence of block size and the Representative Volume Elements (RVE) are discussed, in addition to the influence of anisotropy on the effective Young's modulus.

1 INTRODUCTION

The motivation of this work is to investigate the influence of porosity and void size on the stiffness of 3D geomaterials using a statistical approach. Even if the expected porosity of a site can be conservatively estimated, the location of the voids may be largely unknown such as in geological regions dominated by karstic deposits. This makes a statistical approach appealing. The work presented in this paper is developed from a study of 2D model homogenization of geomaterials containing voids by random fields and finite elements (Griffiths et al. 2012) and 3D random finite element methods (Fenton & Griffiths, 2005). The classic problem of homogenization of heterogeneous materials with variable micro-structure has long been of practical interest to engineers. In the current study, the influence of voids on effective elastic properties is investigated. The goal of homogenization is to predict the effective property of a heterogeneous material, where the effective value is defined as the property that would have led to the same response if the geomaterial had been homogeneous. A useful concept in this homogenization process is the Representative Volume Element (RVE). An RVE is an element of the heterogenous material that is large enough to represent the microstructure but small enough to achieve computational efficiency (e.g. Liu, 2005; Zeleniakiene et al. 2005).

Since the concept of the RVE was first introduced by Hill (1963), several theoretical models have been proposed for dealing with scale effects. Hazanov & Huet (1994) derived results involving mixed boundary conditions, which locate between the static and kinematic uniform boundary conditions for specimens smaller than the size of the RVE. Orthogonal mixed boundary conditions have also been proposed (e.g. Hazanov & Amieur, 1995; Havanov, 1998; Khisaeva & Ostoja-Starzewski, 2006). Numerical methods such as the Finite Element Method (FEM) have also been used to validate the RVE size of random heterogeneous materials. Kanit et al. (2003) used Monte-Carlo simulations to investigate RVE and effective properties, while Zohdi & Wriggers (2001) and Ostoja-Starzewski (2006) investigated the RVE size using a statistical computational approach. Although there are many models developed to investigate the effective properties of a material containing voids, there is no model that works for all problems

(e.g. Böhm, 1998, 2013). See also the reviews published by Torquato (2002), Kachanov (2005) and Klusemann & Svendsen (2009).

In this paper, the Random Finite Element Method (RFEM) (e.g. Griffiths & Fenton 2007), which combines finite element analysis with random field theory, will be used in conjunction with Monte-Carlo simulations, to examine the effective elastic properties of materials with randomly distributed voids. A 3D cube of material, discretized into a relatively fine mesh of 8-node hexahedral elements, forms the basis of the model. Random field theory will be used to generate a material containing intact material and voids with controlled porosity and size. The RFEM can vary the size of the voids through control of the spatial correlation length and excursion theory (see e.g. p.141 in Fenton & Griffiths 2008). For each simulation of the Monte-Carlo process, elements in the mesh are assigned either an intact stiffness value or a much lower stiffness value corresponding to a void. A deterministic analysis follows leading to effective values of the elastic parameters E and υ. Monte-Carlo analyses are typically repeated numerous times until the output statistics of the effective elastic properties (mean and SD) stabilize.

The first part of the paper investigates the size of the RVE for different input void properties. The second part of the paper investigates the statistics of the effective Young's modulus and Poisson's ratio in 3D as a function of porosity and void size, and compares results with numerical and analytical studies by other investigators. Effective properties in 3D are also compared with anisotropic results.

2 FINITE ELEMENT MODEL

Examples of the model which combines elastic material and voids are shown in Figure 1.

The finite element mesh for this study consists of a cubic block of material of side length $L = 50$ modeled by $50 \times 50 \times 50$ 8-node cubic elements of side length $\Delta x = \Delta y = \Delta z = 1.0$. Any consistent system of units could be combined with the dimensions and properties described in this paper. Since a mesh such as this involves rather large global matrices, equation solution in the runs described in this paper will be performed using a Preconditioned Conjugate Gradient (PCG) technique with element-by-element products as described by Smith and Griffiths (2004) which avoids entirely the need to assemble the global stiffness matrix. The model in Figure 2 is subjected to a vertical force $Q = L \times L$ on the top face leading to an average unit pressure on the top face of 1.0. The boundary conditions of the block involve the use of "tied freedoms" that allow analysis of an "ideal" block and direct evaluation of the effective Young's modulus and Poisson's ratio. Tied freedoms

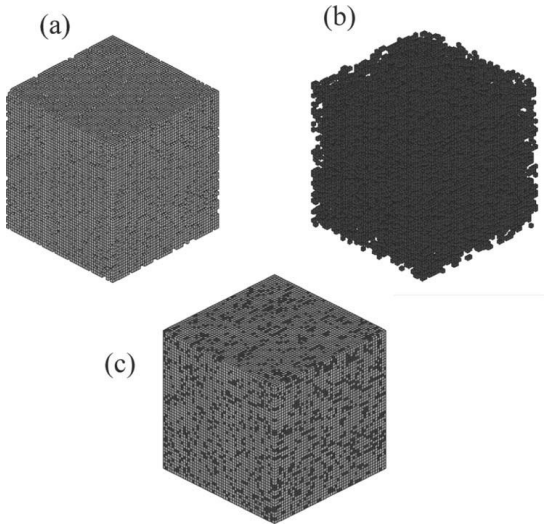

Figure 1. The 3D finite element model of ideal cubic blocks: (a) the solid material, (b) the voids, and (c) the combined model which show dark and light regions indicating voids and solid material respectively.

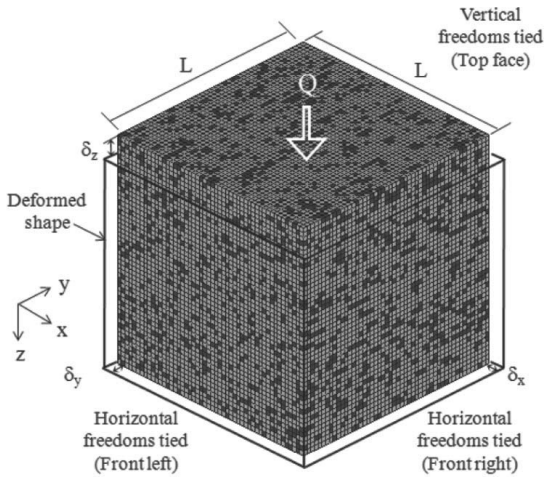

Figure 2. Analysis of tied freedom in a "cubic element test" model with voids. A vertical force is applied on the top side. Rollers are fixed at the bottom and two back sides. The top and the two front sides are tied. The dark and grey elements represent, respectively, void and intact solid elastic material.

are forced to move by the same amount in the analysis. The boundary conditions are such that the cubic block remains a regular hexahedron after deformation. Other methods may give similar outcomes (see e.g. the effects of tied freedom boundary condition from Huang et al. 2013). From this idea, the effective Young's modulus and Poisson's ratio easily be back-figured as will be described.

In particular, the boundary conditions are such that nodes on the base of the block can move only

in the $x - y$ plane. The back left and back right faces are constrained to move only in the $y - z$ and $z - x$ planes respectively. All z-freedoms on the top plane are tied, as are the y-freedoms on the front left plane and the x-freedoms on the front right plane. A consequence of these constraints is that the top surface remaining horizontal and the two front sides remaining vertical following deformation.

These specific boundary conditions enable more direct comparison to be made with experimental results, where displacements may be applied without friction on all sides of the specimen. Periodic boundary conditions have also been used in homogenization studies of heterogeneous media, (e.g. Garboczi & Day, 2005).

3 CONTROLLING POROSITY

The random field generator in the RFEM model known as the Local Average Subdivision method (LAS) (Fenton & Vanmarcke 1990) is used in this paper to model spatially varying voids properties. The target mean porosity n is obtained by using the standard normal distribution shown in Figure 3. A single value of the random variable Z is initially assigned to each element of the finite element mesh. Once the standard normal random field values have been assigned, cumulative distribution tables Φ (suitably digitized in the software) are then used to estimate the value of the standard normal variable $z_{n/2}$ for which

$$\Phi\left(z_{n/2}\right) - \Phi(0) = n/2 \tag{1}$$

where Φ is the cumulative normal distribution function, and n is the target porosity as shown in Figure 3.

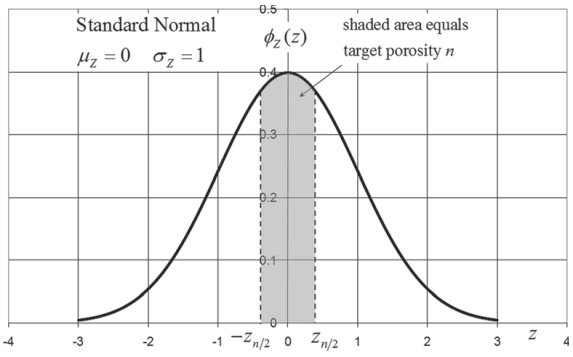

Figure 3. Target porosity area in standard normal distribution of random field. Any element assigned a random field value in the range $|Z| > z_{n/2}$ is treated as intact material a Young's modulus and Poisson's ratio given by $E_0 = 1$ and $\upsilon_0 = 0.3$, respectively.

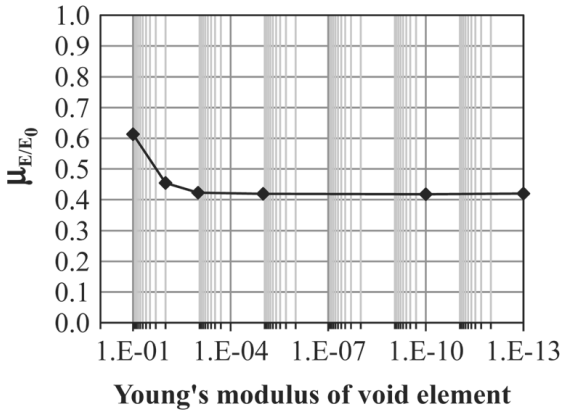

Figure 4. Influence of void element stiffness on the mean effective Young's modulus (intact material, $E_0 = 1$).

Thereafter, any element assigned a random field value in the range $|Z| > z_{n/2}$ is treated as intact material with a Young's modulus and Poisson's ratio given by $E_0 = 1$ and $\upsilon_0 = 0.3$, while any element where $|Z| \le z_{n/2}$ is treated as a void element with Young's modulus and Poisson's ratio given by $E_0 = 0.01$ and $\upsilon_0 = 0.3$ (100 times smaller than the surrounding intact material). As can be seen in Figure 4, for the case when $n = 0.2$, the results show a small influence of the arbitrarily selected Young's modulus of the void elements. In the current work, a void stiffness one hundred times less than the surrounding intact material gave reasonable (and stable) results. The nature of random fields is that the mean porosity is under the user's control, but the porosity of each individual simulation processed by the Monte-Carlo method will vary from one simulation to the next.

4 CONTROLLING OF VOID SIZE

As mentioned previously, two materials with the same average porosity could have quite different void sizes. One model could have frequent small voids, while the other could have less frequent larger voids. The void size in this study is controlled by the random field spatial correlation length θ which incorporates a "Markov" spatial correlation structure as follows

$$\rho = \exp\left(-2|\tau|/\theta\right) \tag{2}$$

where ρ = the correlation coefficient; $|\tau|$ = absolute distance between points in the field; and θ = scale of fluctuation or spatial correlation length. Larger values of θ will lead to larger voids and vice versa.

The Markov equation delivers a spatial correlation that reduces exponentially with distance. For example, from Eq. (3), $\tau < \theta$, the correlation coefficient $\rho > 0.13$. In the current study, the range

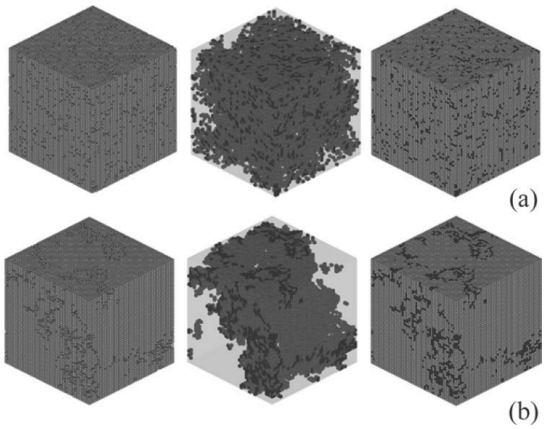

Figure 5. Typical simulations showing generation of voids at (a) low and (b) high spatial correlation lengths θ ($n = 0.2$ in both cases).

of ρ varies from 0 to 1. Points close together are strongly correlated and therefore likely to belong to the same void. In the limiting case of $\theta \to 0$, the random field value changes rapidly from point to point delivering numerous small voids. At the other extreme as $\theta \to \infty$, the random on each simulation becomes increasingly uniform with some simulations representing entirely intact material and other consisting entirely of voids. For example as shown in Figure 5, the models show typical simulations of different void clustering for two materials with the same mean porosity.

5 MONTE-CARLO SIMULATIONS

A "Monte-Carlo" process is combined with the RFEM and repeated until stable output statistics are achieved. The primary outputs from each elastic analysis are the vertical and horizontal deformations of the block δ_z, δ_x and δ_y. Although all simulation use the same θ and n, the spatial location of the voids will different each time. In some cases, the voids may be located just below the top of the block leading to a relatively high δ_z. While in others, the voids may be buried in the middle of the block leading to a relatively low δ_z. Following each simulation, the computed displacements δ_z, δ_x and δ_y are converted into the "effective" values of Young's modulus and Poisson's ratio as follows

Based on Hooke's law,

$$\varepsilon_x = \frac{1}{E}(\sigma_x - \upsilon(\sigma_y + \sigma_z))$$
$$\varepsilon_y = \frac{1}{E}(\sigma_y - \upsilon(\sigma_z + \sigma_x)) \quad (3)$$
$$\varepsilon_z = \frac{1}{E}(\sigma_z - \upsilon(\sigma_x + \sigma_y))$$

Given that L is the side length of cubic block, and assume stress boundary conditions.

$$\sigma_x = 0.0,\ \sigma_y = 0.0\ ,\ \sigma_z = -Q/L^2 \quad (4)$$

$$\varepsilon_x = \frac{\delta_x}{L},\ \varepsilon_y = \frac{\delta_y}{L},\ \varepsilon_z = \frac{\delta_z}{L} \quad (5)$$

hence after substitution into equation (3), the effective elastic properties can be written as

$$E = \frac{Q}{L\delta_z} \quad (6)$$

$$\upsilon_x = \frac{\delta_x}{\delta_z} \quad (7)$$

$$\upsilon_y = \frac{\delta_y}{\delta_z} \quad (8)$$

where E = the effective elastic Young's modulus, Q = stress loading at the top side, υ_x and υ_x = the effective Poisson's ratios based on the displacement in the x- and y-directions respectively.

In each simulation, the effective Young's modulus is normalized as E/E_0 by dividing by the intact Young's modulus E_0. In the current study, following some numerical experiments as shown in Figure 6, it was decided that 1000 simulations for each parametric combination would deliver reasonably repeatable results. In this study, we have expressed the spatial correlation length in dimensionless form

$$\Theta = \frac{\theta}{L} \quad (9)$$

where L is the width of the loaded element ($L = 50$).

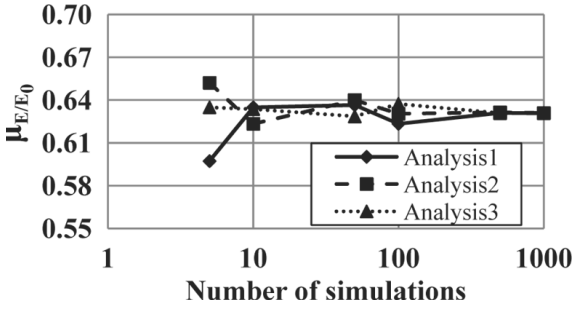

Figure 6. Sensitivity of the mean effective Young's modulus as a function of the number of simulations for $n = 0.2$ and $\Theta = 0.4$. It was decided that 1000 simulations would deliver reasonably repeatability.

6 REPRESENTATIVE VOLUME ELEMENT

An RVE is an element of the heterogeneous material that is large enough to represent the microstructure, but small enough to achieve computational efficiency. The RVE of four cases using the random field 3D finite element model have been considered as shown in Table 1.

Figure 7 shows a sequence of five blocks contained within and including the largest block of $50 \times 50 \times 50$ cubic elements. The different block sizes will indicate the optimal RVE for the given input conditions. When the RVE is "big enough", we expect the standard deviation of the effective Young's modulus to be reduced and its mean essentially constant as shown in Figures 8(a) and 8(b). While the mean values plotted in Figure 8(a) are fairly constant for different block sizes, it could be argued that the block size of $20 \times 20 \times 20$ led to essentially constant values for the low Θ cases (1 and 3), while a larger block, say $30 \times 30 \times 30$ would be needed for stable mean values with the larger Θ cases (2 and 4). The standard deviation shown in Figure 8(b) displays more variability with block size and tends to zero as the blocks get bigger, but at a slower rate for higher values of Θ. In both Figures 8, it is noted that the influence of Θ on block statistics is greater than that of n. The RVE depends more on spatial correlation length than porosity.

Table 1. Different input void properties.

Case	Target porosity (n)	Θ
1	0.2	0.2
2	0.2	0.7
3	0.7	0.2
4	0.7	0.7

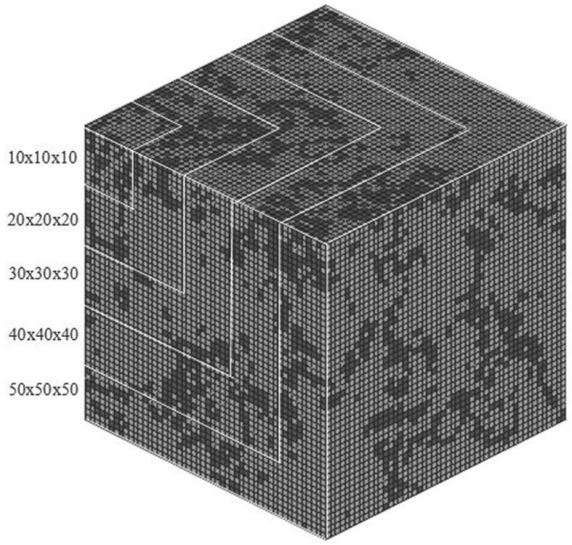

Figure 7. Different block sizes for computing the effective elastic properties of a material with random voids.

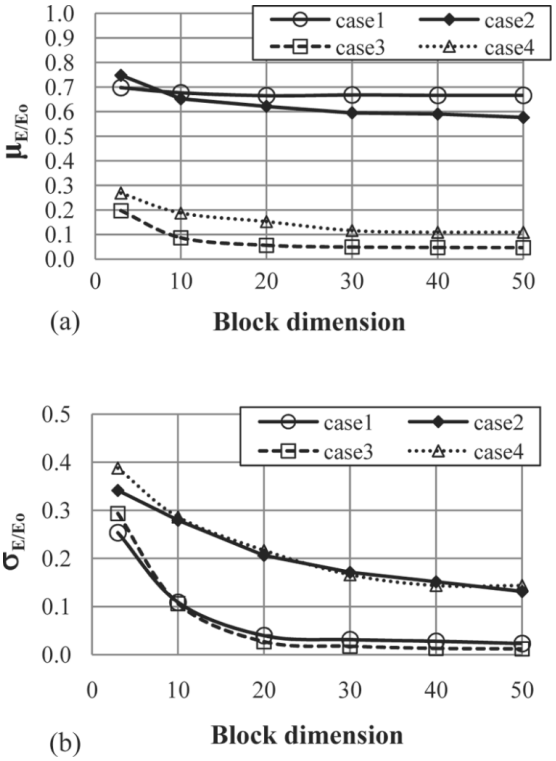

Figure 8. Effective Young's modulus (a) mean and (b) standard deviation following 1000 simulations for different block sizes.

7 RESULTS OF RFEM

Following each set of 1000 Monte-Carlo simulations, the mean and standard deviation of the normalized effective Young's modulus were computed for a range of parametric variations of n and Θ, with results shown in Figures 9 and 10, respectively.

It can be noted from Figure 9 that the mean normalized effective Young's modulus drops towards zero with increasing porosity n and that Θ does not have much influence. Figure 10 shows that Θ has more influence on the standard deviation of the effective Young's modulus σ_{E/E_0}. The standard deviation values as $n \to 0$ (intact stiffness material) and $n \to 1$ (very low stiffness material) show low variance since almost all simulations are the same and model essentially uniform material. The standard deviation was observed to reach a maximum value at around $n \approx 0.4$.

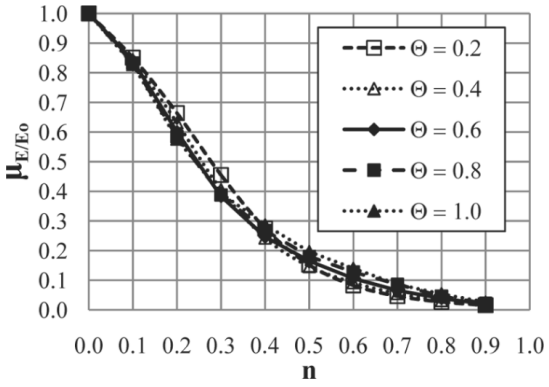

Figure 9. μ_{E/E_0} vs. n for $0.2 \le \Theta \le 1.0$.

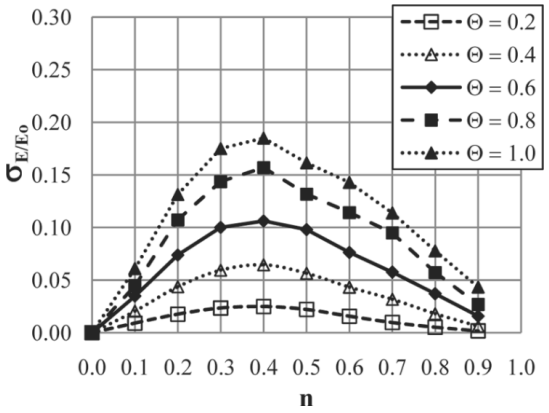

Figure 10. σ_{E/E_0} vs. n for $0.2 \le \Theta \le 1.0$.

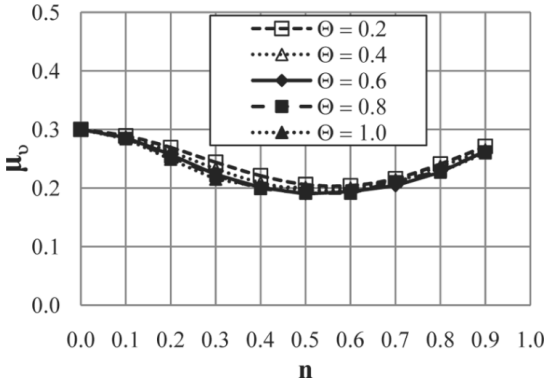

Figure 11. μ_υ vs. n for $0.2 \le \Theta \le 1.0$.

The result obtained from Equations 7 and 8 for the effective Poisson's ratio were in good agreement as expected for the range of n and Θ considered. In the isotropic material model, the two Poisson's ratios are essentially identical after Monte-Carlo simulation; however the results are based on an average to account for any small differences. The plots shown in Figures 11 and 12 give the mean

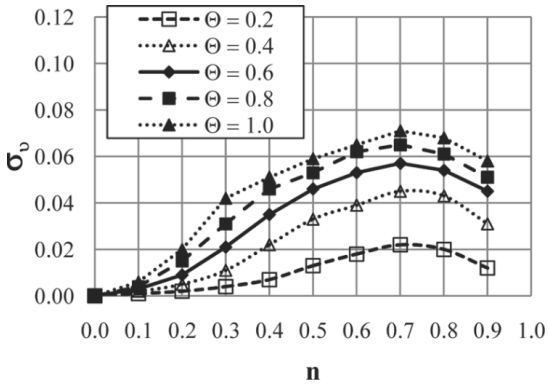

Figure 12. σ_υ vs. n for $0.2 \le \Theta \le 1.0$.

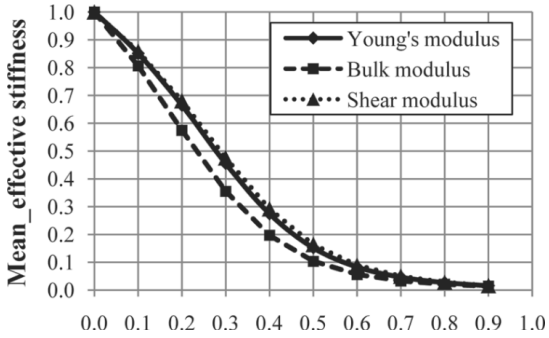

Figure 13. Mean effective values vs. n using $\Theta = 0.2$.

and standard deviation of the effective Poisson's ratio. Figure 11 shows that the mean effective Poisson's ratio μ_υ displays a minimum at around $n = 0.5$. On the other hand, as shown in Figure 12, the standard deviation of Poisson's ratio displays a maximum at $n = 0.7$ which is a similar trend to that observed for Young's modulus in Figure 10. For all values of Θ considered however, the standard deviations were quite small.

Although this paper has focused on Young's modulus and Poisson's ratio, other stiffness moduli may be of interest depending on the context. Figure 13 combines results from Figures 9 and 11 to show the variation of the mean effective shear modulus and bulk modulus using Eqns. (10 and 11). They display a similar trend to that observed for Young's modulus.

$$\mu_K = \frac{\mu_E}{3(1-2\mu_\upsilon)} \tag{10}$$

$$\mu_S = \frac{\mu_E}{2(1+\mu_\upsilon)} \tag{11}$$

where μ_K = the mean effective bulk modulus, μ_S = the mean effective shear modulus.

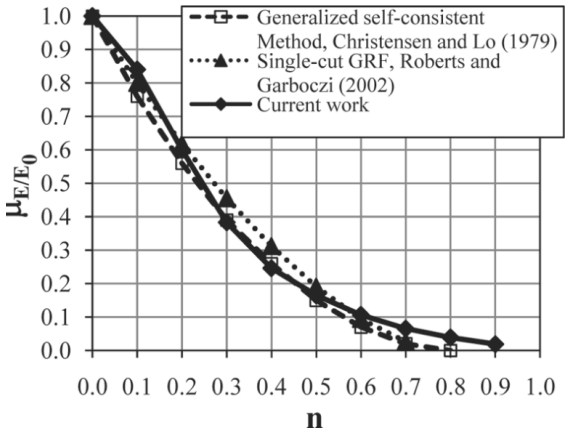

Figure 14. Comparison of the effective Young's modulus obtained from RFEM and other approaches.

8 COMPARISON OF RFEM AND OTHER RESULTS

The theoretical results based on the Generalized Self Consistent Method of Christensen & Lo (1979) and the numerical results based on the single-cut GRF model of Roberts & Garboczi (2002) are compared in Figure 14, with results from the current study using $\Theta = 0.6$ from Figure 9. The Generalized Self Consistent Method involved embedding an inclusion phase directly into an infinite medium. It was demonstrated that the method could also solve the spherical inclusion problem. The single-cut GRF model assigns a random number to each point in space. From Figure 14, it can be observed that the current method gives similar values of the mean effective Young's modulus

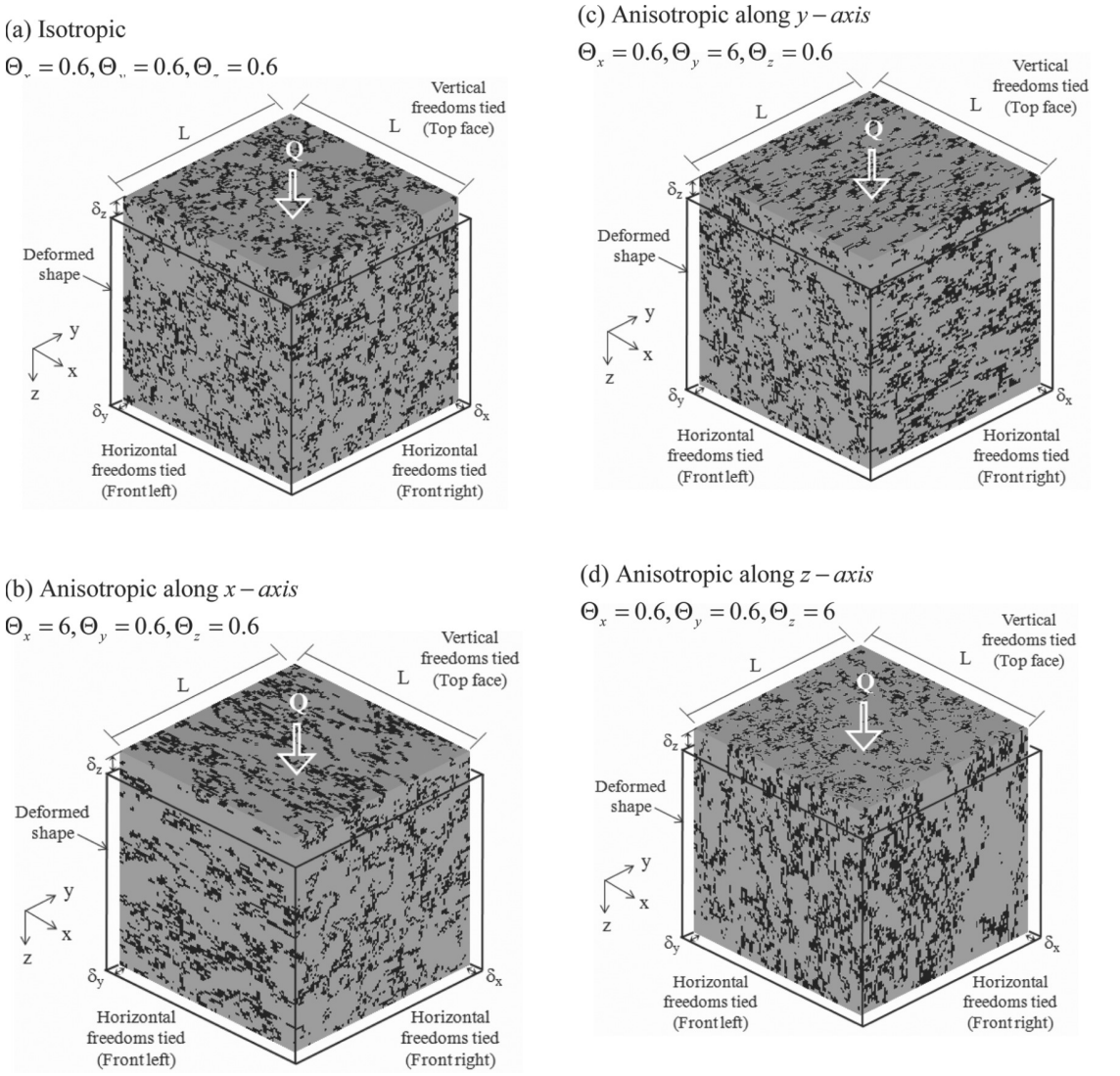

Figure 15. Analysis of tied freedom in four "cubic element test" models with voids: (a) isotropic model, (b) anisotropic model along *x-axis*, (c) anisotropic model along *y-axis* and (d) anisotropic model along *z-axis*.

to those given by the theoretical and numerical methods for all values of n.

9 COMPARISON OF ISOTROPIC AND ANISOTROPIC MODELS

Anisotropic models are performed with different spatial correlation lengths in different directions. Figure 15(a) shows a model of isotropic spatial correlation length at $\Theta_x = \Theta_y = \Theta_z = 0.6$. The voids tend to disperse in all directions within the material. In Figure 15(b), where $\Theta_x = 6$ and $\Theta_y = \Theta_z = 0.6$, and Figure 15(c) where $\Theta_y = 6$ and $\Theta_x = \Theta_z = 0.6$, voids are in horizontally elongated in the x- and y-directions, respectively. On the other hand, in Figure15(d) where where $\Theta_z = 6$ and $\Theta_x = \Theta_y = 0.6$, voids are in vertically elongated in the z-direction. The tied freedom approach described previously continued to be used in all 3D anisotropic models.

Following the Monte-Carlo simulations of the anisotropic models shown in Figure 15, the mean of the effective normalized Young's modulus was compared with isotropic results for a range of n, as shown in Figure 16. It was noted that similar results were obtained when the elongated direction of the anisotropic models was in the x- and y-directions, but the effective Young's modulus was noticeably higher when the elongations were in the z-direction (the direction of loading).

The isotropic 3D results from the current study using $\Theta = 0.6$ are also compared in Figure 16 with 2D (plane strain) for the same spatial correlation length as published previously by Griffiths et al. 2012. The mean normalized effective Young's modulus in 3D is obviously higher than in 2D for the same porosity. A direct comparison between 2D and 3D may not be justified, however, because voids in 2D (plane strain) are like "tunnels" that continue indefinitely into the 3rd dimension, while voids in 3D are isotropic, finite in size, and fully contained within the surrounding material. Thus, it might be explained that the 2D model is actually a 3D model with an infinite spatial correlation length in the 3rd direction.

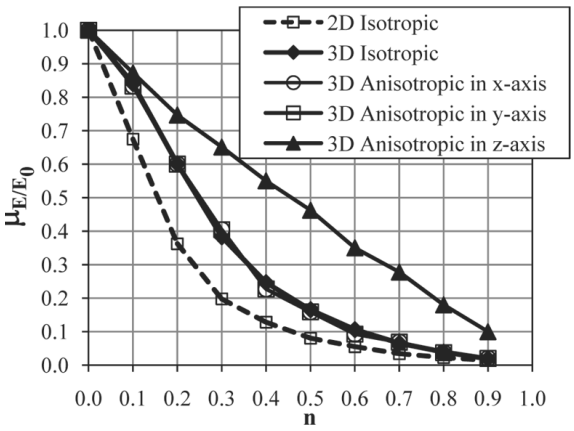

Figure 16. Comparison of the effective Young's modulus obtained from RFEM and other approaches.

10 CONCLUSIONS

A 3D RFEM with "tied freedoms" has been used in this study to investigate the influence of porosity and void size on homogenized elastic properties E and υ. It was observed that while porosity had a significant effect on both the mean and standard deviation of E and υ, the void size had little influence on the mean but more influence on the standard deviation. The study also investigated the RVE needed to capture the essential properties of a heterogeneous material containing voids. It was found that for the same porosity, the larger the size of the voids, the greater the size of the RVE. Finally, the paper presented favorable comparisons of the effective elastic properties in 3D with those obtained analytically and numerically by other investigators. In addition, the effective Young's modulus of the anisotropic system depends on the direction of voids elongation. The stiffest case was observed when the direction of void elongation was in the same direction as the loading. The RFEM approach to homogenization described in this paper shows much promise, and opens the possibility of making probabilistic statements about engineering performance of heterogeneous geomaterials. The probabilistic aspect has not been discussed in the current paper, but remains an area of continued research.

ACKNOWLEDGEMENT

The authors wish to acknowledge the support of (i) NSF grant CMMI-0970122 on "GOALI: Probabilistic Geomechanical Analysis in the Exploitation of Unconventional Resources", and (ii) The Royal Thai Government for their support of the second author.

REFERENCES

Böhm, H.J. 1998, 2013. A short introduction to basic aspects of comtinuum micromechanics, TU Wien, Vienna.

Christensen, R.M. and Lo, K.H. 1979. Solutions for effective shear properties in three phase sphere and cylinder models. *J. Mech. Phys. Solids* 27: 315–330.

Fenton, G.A. & Griffiths, D.V. 2005. Three-Dimension Probabilistic Foundation Settlement. *J. Geotech. Geoenviron. Eng.* 131 (2): 232–239.

Fenton, G.A. & Griffiths, D.V. 2008. Risk Assessment in Geotechnical Engineering, John Wiley & Sons, Hoboken, NJ.

Fenton, G.A. & Vanmarcke, E.H. 1990. Simulation of random fields via local average subdivision. *J Eng. Mech. 1*16 (8): 1733–1749.

Garboczi, E.J. & Day, A.R. 2005. An algorithm for computing the effective linear elastic properties of heterogeneous materials: three-dimensional results for composites with equal phase Poisson ratios. *J. Mech. Phys. Solids* 43 (9): 1349–1362.

Griffiths, D.V. & Fenton, G.A. 2007. Probabilistic Methods in Geotechnical Engineering, CISM Courses and Lectures No. 491, Pub. Springer, Wien, New York.

Griffiths, D.V., Paiboon, J., Huang, J. & Fenton, G.A. 2012. Homogenization of geomaterials containing voids by random fields and finite elements. *Int. J. Solids Structure* 49: 2006–2014.

Hazanov, S. & Huet, C. 1994. Order Relationships for Boundary-Conditions Effect in Heterogeneous Bodies Smaller Than the Representative Volume. *Journal of the Mechanics and Physics of Solids* 42 (12): 1995–2011.

Hazanov, S. & Amieur, M. 1995. On overall properties of elastic heterogeneous bodies smaller than the representative volume. *International Journal of Engineering Science* 33 (9): 1289–1301.

Hazanov, S. 1998. Hill condition and overall properties of composites. *Archive of Applied Mechanics* 68 (6): 385–394.

Hill, R. 1963. Elastic properties of reinforced solids: some theoretical principles. *J. Mech. Phys. Solids* 11: 357–372

Huang, J.S., Krabbenhoft, K. & Lyamin, A. 2013. Statistical homogenization of elastic properties of cement paste based on X-ray microtomography images. *Int. J. Solids Structure* 50: 699–709.

Kachanov, M. & Sevostianov, I. 2005. Onquantitative characterization of microstructures and effective properties. *Int. J. Solids Struct.* 42: 309–336.

Kanit, T., Forest, S., Galliet, I., Mounoury, V. & Jeulin, D. 2003. Determination of the size of the representative volume element for random composites: statistical and numerical approach. *Int. J. Solids Structure* 40 (13–14): 3647–3679.

Khisaeva, Z.F. & Ostoja-Starzewski, M. 2006. On the size of RVE in finite elasticity of random composites. *Journal of Elasticity* 85 (2): 153–173.

Klusemann, B. & Svendsen, B. 2009. Homogenization methods for multi-phase elastic composites: Comparisons and benchmarks. *Technische Mechanik* 30 (4): 374–386.

Liu, C. 2005. On the minimum size of representative volume element: an experimental investigation. *Exp. Mech. 4*5 (3): 238–243.

Ostoja-Starzewski, M. 2006. Material spatial randomness: From statistical to representative volume element. *Probabilistic Engineering Mechanics* 21 (2): 112–132.

Roberts, A.P. & Garboczi, E.J. 2002. Computation of the linear elastic properties of random porous materials with a wide variety of microstructure. *Proc. Royal Soc. of London* 458 (2021): 1033–1054.

Smith, I.M. & Griffiths, D.V. 2004. *Programming the finite element method*, John Wiley and Sons, Chichester, New York, 4th edition

Torquato, S. 2002. Random heterogeneous materials: microstructure and macroscopic properties. Springer-Verlag, NY.

Zeleniakiene, D. Griskevicius, P. & Leisis, V. 2005. The comparative analysis of 2D and 3D microstructural models stresses of porous polymer materials. ISSN 1392-1207. Mechanika, Nr. 3 (53).

Zohdi, T.I. & Wriggers, P. 2001. Aspects of the computational testing of the mechanical properties of microheterogeneous material samples. *International Journal for Numerical Methods in Engineering* 50 (11): 2573–2599.